Cognitive Neural Network Driving DoF-Scalable Limbs in Time-Evolving Situations

Carlos Calvo Tapia
Instituto de Matemática Interdisciplinar,
Facultad de CC. Matemáticas
Universidad Complutense de Madrid

José Antonio Villacorta-Atienza
Instituto de Matemática Interdisciplinar,
Biomathematics Unit
BEE Department, Faculty of Biology
Universidad Complutense de Madrid

Innokentiy Kastalskiy
Lobachevsky State University
Gagarin Ave. 23, 603950
Nizhny Novgorod, Russia

Sergio Diez-Hermano
Biomathematics Unit
BEE Department, Faculty of Biology
Universidad Complutense de Madrid

Abel Sánchez-Jiménez
Instituto de Matemática Interdisciplinar
Biomathematics Unit
BEE Department, Faculty of Biology
Universidad Complutense de Madrid

Valeri A. Makarov
[1]Instituto de Matemática Interdisciplinar
Universidad Complutense de Madrid
Av. Complutense s/n, 28040, Madrid, Spain
[2]Lobachevsky State University
Gagarin Ave. 23, 603950
Nizhny Novgorod, Russia
E-mail: vmakarov@ucm.es

***Abstract*—Object handling and manipulation are vital skills for humans and autonomous humanoid robots. The fundamental bases of how our brain solves such tasks remain largely unknown. Here we develop a novel approach that addresses the problem of limb movements in time-evolving situations at an abstract cognitive level. We exploit the concept of generalized cognitive maps constructed in the so-called handspace by a neural network simulating a wave simultaneously exploring different subject actions, independently on the number of objects in the workspace. We show that the approach is scalable to limbs with minimalistic and redundant numbers of degrees of freedom (DoF). It also allows biasing the effort of reaching a target among different DoF.**

I. Introduction

The effective and efficient object handling and manipulation are vital for humans' daily life. In this context, the sensory-motor abilities ordinarily exhibited by humans may appear simple at first glance. However, many of them, e.g., playing ping-pong, require forecasting the future states of different objects in the environment, their matching with feasible body movements, and selecting optimal strategies. The intrinsic complexity of these simple-but-difficult tasks impedes modern robots to mimic smoothly even basic human sensory-motor skills in real-life scenarios.

An extensive literature suggests that a purely programmatic approach to the problem of limb movement can only work in tailor-made scenarios [1]. It is not robust to changes in the environment and requires complete rebuilding if, e.g., we try to transfer mathematical methods developed for a manipulator with minimal number of degrees of freedom (DoF) to a redundant one [2]. Thus, the problem of effective manipulation of objects requires support at an abstract cognitive level.

Growing experimental evidence suggests that mammals, and humans in particular, use an internal representation of the environment and their body for movement planing and execution [3]–[8]. Such a representation can be implemented in the form of *cognitive maps*, which provide an abstract description of the environment. A cognitive map structures relevant geometric information and rules on how a subject can act in a given situation. Usually it offers multiple solutions, which allows selecting different strategies to accomplish the goal [8]–[10]. However, the concept of cognitive maps is limited to the description of static situations [11]. When a scenario rapidly changes in time, creating individual cognitive maps for each time frame becomes unfeasible.

Existing works dealing with manipulators usually exploit one of the following paradigms: 1) The potential field method, originally putted forward by Khatib [12]–[14]; 2) The technique based on learning from demonstration [15]–[17]; 3) The dynamical system approach based on construction of attractors and repellers in a phase space [18]; and 4) The neural network approach for solving the kinematic problem [19], [20]. Despite important results recently obtained, still most of the works deal with either static or quasi-static situations and pay little attention to the cognitive abilities of the developed solutions. Moreover, frequently the provided approaches have a limited level of abstraction and hence lack scalability or portability.

In this work, we develop a general neural network approach implementing the concept of cognitive maps for a versatile controlling of limbs in time-evolving situations. The approach provides a robust scalable solution and is applicable to limbs with minimalistic and redundant number of DoF. It also allows setting a constraint that can bias efforts in target reaching among different DoF.

Earlier, we generalized the notion of cognitive maps into time-evolving situations and introduced the so-called *generalized cognitive maps* (GCMs) [11], [21]. Briefly, a GCM is

978-1-5090-6014-6/18/$31.00 ©2018 IEEE

built by a wave propagating in a neural network that models all possible subject's movements. The wave extracts the relevant spatiotemporal events from the environment and projects them into a purely spatial map. Thus, the explicit time dimension disappears and we get a static representation that can further be used for path planing and execution, like an ordinary cognitive map [22], [23].

The original procedure of building GCMs [11] assumes that the subject (human or robot) has a rigid body, i.e., there are no internal degrees of freedom. Then, the essential spatial extension and changing geometry of a limb bring an additional degree of complexity. Thus, GCMs cannot be applied straightforwardly to control limb movements. To resolve this problem, recently we have proposed a transformation from a workspace to a new space, which allows extending the GCM-theory into limbs with minimalistic DoF [24], [25]. In the new task or the so-called handspace [26] we can easily build GCMs and trace global collision-free trajectories for limb movements. In this work, we further develop and generalize the GCM concept and apply it to limbs with minimalistic and redundant DoF.

II. The Problem

Figure 1 illustrates a kinematic model of an upper limb consisting of three segments moving in a two-dimensional *workspace*, $\mathcal{W} \subset \mathbb{R}^2$. The limb shoulder is fixed at the origin of the (x_1, x_2)–plane and it is joined to an articulated elbow by a rigid segment of length ρ. A forearm of length l joins the elbow with the hand located at $\vec{x}_h \in \mathcal{W}$. The wrist can bend, thus changing the angle of the last limb segment of length h.

To simplify further calculations, we rescale the spatial coordinates in such a way that the length of the forearm is $l = 1$ a.u. We then restrict the limb's workspace to:

$$\mathcal{W} = \overline{\mathcal{B}}_{\rho+1+h} \setminus \{\vec{0}\} \subset \mathbb{R}^2, \tag{1}$$

i.e., to a disk of radius $(\rho+1+h)$ centered at the origin (here and further on, $\overline{\mathcal{B}}_r$ denotes a closed disk of radius r centered at the origin).

The shoulder, elbow, and wrist joints can freely rotate within specific angular limits that depend on the internal limb structure. Thus, we have 3 DoF in a 2D workspace and hence the upper limb has redundant DoF. Our goal is to touch by the last segment (hand) a target avoiding collisions with obstacles.

Figure 1 illustrates a simple situation with a point target and a point obstacle, marked by $\vec{x}_t$ and $\vec{x}$, respectively. Further, we will generalize this setting into a situation with multiple *moving* targets and obstacles of arbitrary shapes. We also note that the target cannot be touched by the upper arm and forearm, i.e., it plays the role of an obstacle for these segments of the limb.

We now aim at providing a neural network model capable of driving the limb in different time-evolving situations. For example, the limb should kick a falling ball and simultaneously avoid collisions with other, in general moving, objects. The model will implement an approach based on construction of Generalized Cognitive Maps [11], [24], [25]. To build a GCM, we simultaneously perform [11]: i) prediction of the object movements and ii) simulation of all possible subject actions and matching them with the object movements. Both calculations are performed "mentally" in neural networks and must be done significantly faster than the time scale of the dynamic situation (for more details, see [23]). Thus, in what follows we will deal with two times: 1) t is the "real" time in the workspace $\mathcal{W}$, and 2) τ is the "mental" time used in mental calculations made by the neural networks in $\mathcal{H}$. A sufficiently fast calculation in mental time τ can be achieved either by a parallel computation in hardware or through learning process (for more details, see [22]). Then, having a solution in $\mathcal{H}$, we can rescale time τ to implement a real movement in $\mathcal{W}$.

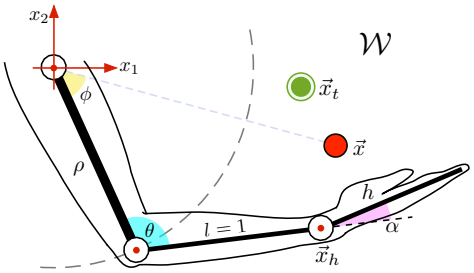

Fig. 1. Model of an upper limb with 3 DoFs in a 2D workspace $\mathcal{W}$. The shoulder is fixed at the origin. The upper arm, forearm, and hand have lengths ρ, $l = 1$, and h a.u., respectively. The upper arm forms the angle ϕ with the direction to the point-like obstacle located at $\vec{x}$ (red circle). The forearm has the angle θ with the upper arm, and α is the angle of the hand. The limb segments can freely rotate within specific limits (around red points in open circles). The goal is to reach the target at $\vec{x}_t$ (green circle) by the hand avoiding collisions.

III. Handspace Transformation

To enable the use of generalized cognitive maps, we first have to eliminate the limb spatial dimensions and rotational degrees of freedom. This allows representing the limb as a point in some equivalent space. Let us now introduce the so-called *handspace* [24], [25]:

$$\mathcal{H}_3 = \left(\overline{\mathcal{B}}_{1+\rho} \setminus \mathcal{B}_{\max\{0,1-\rho\}}\right) \times J \subset \mathbb{R}^3, \tag{2}$$

where $J = [\alpha_{\min}, \alpha_{\max}]$ is the feasible interval of the wrist angles. We note that the hand location and angle belong to this space, i.e., $(x_h, \alpha) \in \mathcal{H}_3$. In general, $\mathcal{H}_3$ is a cylinder with a hole in the center. For the sake of simplicity and without loss of generality, in what follows, we assume $\rho \geq 1$. Then, $\mathcal{H}_3$ is a cylinder without the line segment in the center $\{(0,0)\} \times J$.

Note that $\dim(\mathcal{H}_3) = 3 > \dim(\mathcal{W}) = 2$ and hence we deal with a limb with redundant DoF. We can also consider a reduction of the handspace (2) to two dimensions: $\mathcal{H}_2 = \mathcal{H}_3(\alpha^*)$. In this case the hand angle (Fig. 1) is fixed $\alpha = \alpha^*$, i.e., the wrist is rigid and the limb is minimalistic [DoF $= \dim(\mathcal{W})$]. Then, $\mathcal{H}_2$ is a disk without a point at the origin.

The technique to introduce a mapping from $\mathcal{W}$ to $\mathcal{H}_2$ has been described elsewhere [24], [25]. Here we briefly summarize the earlier result and provide its extension to a 3D case. Without loss of generality, let us first assume that there exists a point-like target and a point-like obstacle in $\mathcal{W}$ (Fig. 1, green and red circles, respectively).

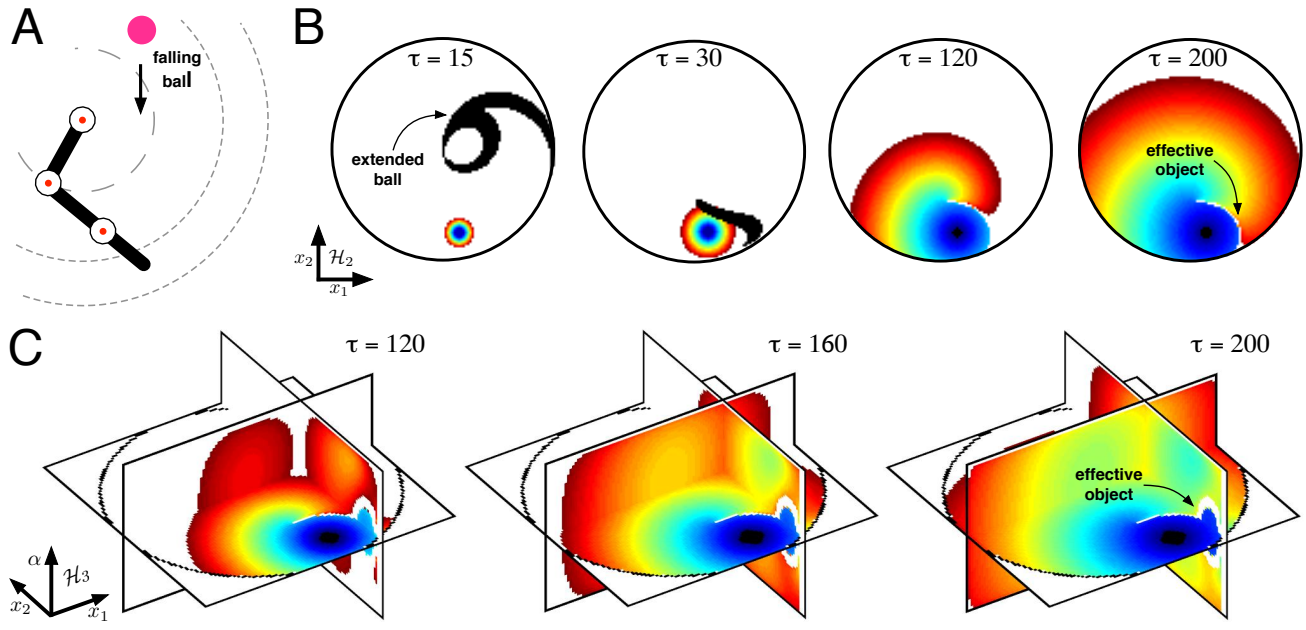

Fig. 2. Wave exploration of the handspace for a dynamic situation. A) Simple dynamic situation. A hand (last segment of the limb shown in black) should kick a falling ball (in pink). The limb can have either 2 DoF (i.e., the wrist joint is fixed) or 3 DoF (the wrist is flexible). Gray dashed circles mark regions reachable by different segments. B) The process of generation of a generalized cognitive map for the limb with 2 DoF in the hand space $\mathcal{H}_2$. Successive snapshots illustrate a traveling wavefront exploring the environment (colored region) and the extended object corresponding to the falling ball (in black, snapshots $\tau = 15$, $\tau = 30$). The wave generates a potential field (colors from blue to red) and an effective object (in white, snapshot $\tau = 200$). C) The same as in (B) but for the limb with 3 DoF in the hand space $\mathcal{H}_3$.

A. Compaction of Limb

The mapping of the limb is given:

$$\begin{array}{rccc} C: & \mathcal{P}(\mathcal{W}) & \rightarrow & \mathcal{H}_3 \\ & \mathcal{L} & \mapsto & C(\mathcal{L}) = (\vec{x}_h, \alpha), \end{array} \tag{3}$$

where $\mathcal{L} \subset \mathcal{W}$ represents the union of the upper arm, forearm, and hand segments. Thus, the whole limb is reduced to a single point located at $(\vec{x}_h, \alpha)$ in the handspace $\mathcal{H}_3$. Note that if α is fixed (rigid wrist) we get a mapping to $\mathcal{H}_2$.

B. Extension of Objects

While the limb is mapped into a point in the handspace, the mapping of objects goes in opposite way. A point-like object is extended into a set of curves in $\mathcal{H}_2$ and into a set of surfaces in $\mathcal{H}_3$. Each curve or surface corresponds to collisions of the point object with different points along a given segment of the limb. Geometrically, such an extended object represents the locus of wrist locations and hand angles while the limb slides around the obstacle in the workspace.

To illustrate such a situation in $\mathcal{H}_2$, let us consider a limb actuating in a dynamic situation: a ball moves in the workspace (Fig. 2A). Then, for each time instant t, the ball occupies different positions in the workspace $\mathcal{W}$. Figure 2B (black areas in snapshots corresponding to mental time $\tau = 15$ and $\tau = 30$) illustrates the changing shape and the displacement of the extended ball in $\mathcal{H}_2$. Similar but even more evolved representations of the extended 3D object can be obtained in $\mathcal{H}_3$.

Let us now describe the mapping. We consider a point object located at some fixed t at $x \in \mathcal{W}$. Then the map extending the point can be expressed as:

$$\begin{array}{rccc} E: & \mathcal{W} & \rightarrow & \mathcal{P}(\mathcal{H}_3) \\ & x & \mapsto & E(\vec{x}). \end{array} \tag{4}$$

Since the object can collide with tree limb segments, the image will be given by $E(\vec{x}) = E_1(\vec{x}) \cup E_2(\vec{x}) \cup E_3(\vec{x})$, where $E_{1,2,3}$ represent the extensions due to collisions with the upper arm, forearm, and hand, respectively. Note that depending on the position of the object x, some of E_j can be empty (e.g., if $x \notin \overline{\mathcal{B}}_\rho$, then $E_1(\vec{x}) = \emptyset$).

1) Extension due to collision with upper arm: If the object is reachable by the upper arm, a contact with this segment can take place whenever $\phi = 0$. Thus, we obtain the expansion:

$$E_1(\vec{x}) = \{F_1(\theta, \vec{x}) : \theta \in [0, \pi]\} \times J, \tag{5}$$

where

$$F_1(\theta, \vec{x}) = \mathcal{M} \begin{pmatrix} \rho - \cos\theta \\ \sin\theta \end{pmatrix} \tag{6}$$

and

$$\mathcal{M} = \frac{1}{\|\vec{x}\|} \begin{pmatrix} x_1 & -x_2 \\ x_2 & x_1 \end{pmatrix}, \quad \vec{x} = (x_1, x_2)^T \tag{7}$$

is the rotation matrix. Note that the constraint on θ in (5) is imposed by assuming that the elbow joint can rotate in the limits $[0, \pi]$ (a human-like limb). Otherwise it can be relaxed.

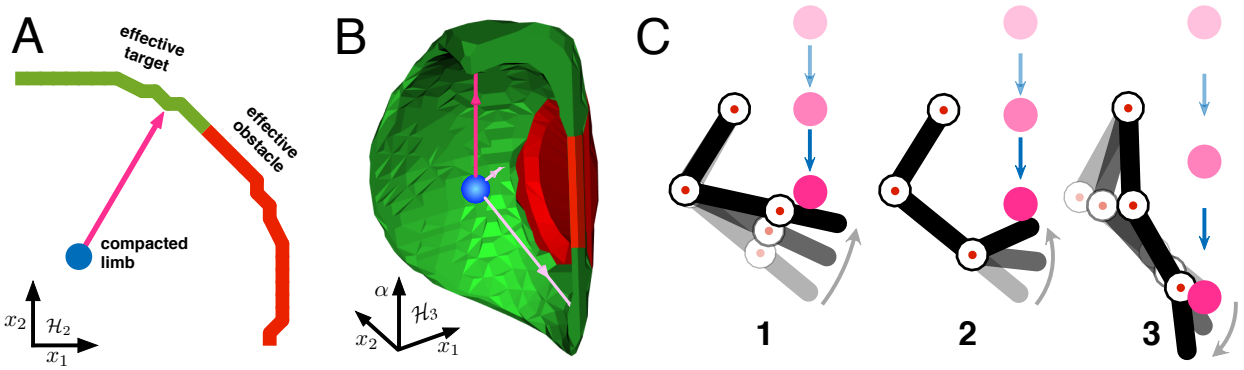

Fig. 3. Effective static objects and execution of limb movement for the situation shown in Fig. 2. A) Effective object in $\mathcal{H}_2$ (amplified from Fig. 2B, $\tau = 200$) contains two parts: effective target (in green) and effective obstacle (in red). B) Same as in (A) but in $\mathcal{H}_3$. C) Three representative examples of limb movements receiving the ball with significantly different hand angles. The movement shown in Panel 1 can be implemented in a 2-DoF manipulator, whereas Panels 1–3 are available for a 3-DoF manipulator.

2) Extension due to collision with forearm: Let us assume that the object is reachable by the forearm. Then, its expansion is given by:

$$E_2(\vec{x}) = \{F_2(\phi, \vec{x}) : \phi \in [-\phi_{\max}, 0]\} \times J, \tag{8}$$

where

$$F_2(\phi, \vec{x}) = \frac{\vec{x}}{\lambda_{\vec{x}}(\phi)} - \rho \left[\frac{1}{\lambda_{\vec{x}}(\phi)} - 1\right] \mathcal{M} \begin{pmatrix} \cos\phi \\ \sin\phi \end{pmatrix} \tag{9}$$

and

$$\lambda_{\vec{x}}(\phi) = (\rho^2 + \|\vec{x}\|^2 - 2\rho\|\vec{x}\| \cos\phi)^{\frac{1}{2}} \tag{10}$$

is the distance between the elbow and the object. Note that $\phi \leq 0$ and $\lambda_{\vec{x}}(\phi) \leq 1$. The lower bound for ϕ in (8) is given by

$$\phi_{\max}(\vec{x}) = \arccos\left(\frac{\rho^2 + \|\vec{x}\|^2 - 1}{2\rho\|\vec{x}\|}\right). \tag{11}$$

3) Extension due to collision with hand: Assuming that the hand has an angle $\alpha \in J$ and is in contact with the object at a distance $d = \|\vec{x} - \vec{x}_h\| \leq h$, then the expansion of the object is given by

$$E_3(\vec{x}) = \{F_3(d, \alpha, \vec{x}) : d \in [d_{\min}, h], \alpha \in J\}, \tag{12}$$

where

$$F_3(d, \alpha, \vec{x}) = \vec{x}_e + \frac{\text{sign}(\alpha)}{\beta_{\vec{x}}\|\vec{x} - \vec{x}_e\|} (I_2 + dR_\alpha)(\vec{x} - \vec{x}_e), \tag{13}$$

R_α is the standard clockwise rotational matrix,

$$\beta_{\vec{x}} = (1 + d^2 + 2d\cos\alpha)^{\frac{1}{2}} \tag{14}$$

is the distance between the elbow and the object, and

$$\vec{x}_e = \frac{1}{2\|\vec{x}\|} \mathcal{M} \begin{pmatrix} \|\vec{x}\|^2 + \rho^2 - \lambda_{\vec{x}}^2 \\ -\left[(2\|\vec{x}\|\rho)^2 - (\|\vec{x}\|^2 + \rho^2 - \lambda_{\vec{x}}^2)^2\right]^{\frac{1}{2}} \end{pmatrix}. \tag{15}$$

The lower bound for d in (12) is given by

$$d_{\min}(\alpha, \vec{x}) = \left[(\|\vec{x}\| - \rho)^2 - \sin^2\alpha\right]^{\frac{1}{2}} - \cos\alpha \tag{16}$$

if it is positive, or $d_{\min} = 0$ otherwise.

Finally, when dealing with a real object of an arbitrary shape, the transformation (4) is applied to the object's boundary. This generates extended objects occupying areas in $\mathcal{H}_2$ (see, e.g., Fig. 2B, panel $\tau = 15$, in black) or volumes in $\mathcal{H}_3$ (not shown in Fig. 2C for visual clarity).

IV. Exploration of Handspace and Generalized Cognitive Maps

As mentioned above, to construct a GCM we perform: i) prediction of the objects' movements and ii) simulation of all possible subject's actions matched with the objects' movements. There are several ways to solve the first problem (see, e.g., [11], [22], [24]). For the sake of simplicity, here we assume that the trajectories of all objects are given and hence we will concentrate on solving the second, much more complex task.

Using the predicted trajectories of objects in the workspace, we can evaluate for each time instant τ their extended images in the handspace (Fig. 2B, black areas). Then, we can simulate all possible hand movements by a wave (see, for details, [11], [22]). In the handspace $\mathcal{H}_3$, the wave is initiated at the location of the wrist and the initial hand angle $(\vec{x}_h(0), \alpha(0))$, whereas in $\mathcal{H}_2$ it starts from $\vec{x}_h(0)$ ($\alpha = 0$). Figures 2B and 2C illustrate the process of wave propagation in $\mathcal{H}_2$ and $\mathcal{H}_3$, respectively.

The set of points on the wavefront represents all possible configurations of the limb (wrist location and hand angle) at time τ. If the wavefront collides with an extended object, then such an event corresponds to a possible collision of the limb and the object. Then, we create in the handspace *effective static objects* at the locations of such collisions.

Figures 3A and 3B illustrate the shapes of the effective static objects obtained in $\mathcal{H}_2$ and $\mathcal{H}_3$, respectively (see also Figs. 2B and 2C, panels $\tau = 200$). In both cases, one part of the effective object (shown in green) corresponds to a target, i.e., to collisions of the ball with the hand in the workspace, while the other one (shown in red) marks collisions of the ball with forearm. Thus, the effective static objects should be either avoided (obstacles) or reached (targets). Using the potential

field (Figs. 2B, 2C, $\tau = 200$) and the effective objects (Figs. 3B, 3C), we can trace different trajectories to the target.

Let us now implement the wave process leading to formation of effective objects and a potential field guiding the limb.

A. Simulation of Possible Subject Actions

In earlier works, we considered 2D internal representations of workspaces and postulated a constant velocity c for the explorative wave [11], [24], [25]. This is equivalent to considering the handspace $\mathcal{H}_2$ of the limb with a rigid wrist. Then, the velocity of the wrist $\vec{v} = d\vec{x}_h/dt \in \mathbb{R}^2$ satisfies $\|\vec{v}\| = c$ (implementing, e.g., maximally fast displacement).

Now we take into account the rotation of the wrist joint with an angular velocity $\omega = d\alpha/dt \in \mathbb{R}$. Then, we impose the following constraint on the compound velocity:

$$\|\vec{v}\|^2(t) + \gamma_0 \omega^2(t) = c^2, \tag{17}$$

where γ_0 is the bias between the velocity of motions in (x_1, x_2)–plane and rotation of the wrist. Note that such a formulation is similar to fixing the kinetic energy of the limb.

To account for constraint (17) in the handspace $\mathcal{H}_3$, we design a neural network in the form of a 3D cylindrical lattice:

$$\Lambda = \left\{(i,j,k) \in \mathbb{Z}^3 :\ i^2 + j^2 \le r^2,\ 1 \le k \le K\right\}, \tag{18}$$

where the constant $r \in \mathbb{N}$ defines the spatial resolution in (x_1, x_2) and is linked with the value $(\rho + 1)$; $K \in \mathbb{N}$ defines the resolution for the wrist bending, linked with $|J|$.

On the lattice Λ we define the following dynamical system:

$$\frac{du_I}{d\tau} = q_I\big(f(u_I) + d_0(\Delta_x + \gamma\Delta_\alpha)u_I\big), \tag{19}$$

where $I = (i,j,k) \in \Lambda$; u_I is the membrane potential of neuron I; Δ_x, Δ_α are the discrete Laplacians in the corresponding variables; and $f(u) = u(u - 0.1)(1 - u)$ is the cubic nonlinearity, selected to ensure propagation of waves in the lattice. The binary function $q_I(\tau) \in \{0, 1\}$ describes formation of effective objects and will be discussed later. The diffusion coefficient d_0 can be adjusted to account for the velocity of the arm movements in the workspace c and the velocity bias

$$\gamma = \gamma_0 \frac{(\rho + 1)^2 K^2}{r^2 |J|^2}. \tag{20}$$

We note that for $\gamma = 0$ Eq. (19) is reduced to the system on a disk (e.g., in $\mathcal{H}_2$). It corresponds to movements with a rigid wrist joint. Thus, model (19) generalizes our previous developments restricted to $\mathcal{H}_2$ [24], [25]. The other limit $\gamma \to \infty$ and $d_0\gamma = \text{const}$ corresponds to the situation where the wrist bending is the only available movement, i.e., we force the upper arm and forearm to stay immobile.

The dynamical system (19) is considered with Neumann boundary conditions (on the cylinder and extended objects). At the beginning the neurons are set to $u_I(0) = 0\ \forall I \in \Lambda \setminus L$, $u_I(0) = 1\ \forall I \in L$, where L is a small spheroid region centered at the initial hand position $I_h(0)$ [counterpart of $(\vec{x}_h(0), \alpha(0))$] and with the eccentricity defined by γ. Such an initial condition ensures correct formation of a spheroid wavefront at the beginning of integration of (19). We also note that $q_I(\tau) = 0\ \forall I \in L$ and hence $u_I(\tau) = 1\ \forall \tau \ge 0$.

B. Formation of Effective Static Objects

At $\tau > 0$, a wavefront propagates in the lattice (19) and switches cells from the initial downstate ($u_I = 0$) to the upstate ($u_I = 1$). Figures 2B and 2C show the wavefront simulating the same dynamic situation (Fig. 2A), but in $\mathcal{H}_2$ and $\mathcal{H}_3$, respectively. The time instant $\tau = b_I$ when cell I crosses a threshold (i.e., $u_I(b_I) = u_{\text{th}}$) is stored. Thus, behind the wavefront we obtained a potential field:

$$G = \{b_I\}, \quad I \in \Lambda, \tag{21}$$

(color coded in Figs. 2B, 2C).

The circular shape (spheroid in $\mathcal{H}_3$) of the wavefront at the beginning (Fig. 2B, $\tau = 15$) means that the hand can move equally well in all directions. However, this circular shape is broken once the wave approaches an extended object (Fig. 2B, $\tau = 30$). Such events correspond to possible collisions of the limb with the object. Part of these represent collisions with the forearm and the others with the hand (Figs. 3A and 3B). The former should be avoided, whereas the latter is desired (the hand kicks the target in mental simulation).

We note that the process of collision of the wave with an extended object technically is similar in $\mathcal{H}_2$ and $\mathcal{H}_3$. However, in the latter case, the wave propagates in 3D and the resulting collisions can produce much more evolved forms, in general not reducible to $\mathcal{H}_2$.

Let us now provide mathematical details for the process of formation of effective obstacles in the neural network (19). It is convenient to introduce the discrete mental time $n = 0, 1, \ldots$ related to the continuous time by $\tau = hn$, where h is the integration time step. Then, we denote by Γ_n the set of cells $\{I\} \subset \Lambda$ occupied by the extended objects at time instant n in the hand space and define the following iterative process:

$$\begin{aligned} &\Omega(0) \leftarrow \emptyset \\ &\Omega_n \leftarrow \Omega_{n-1} \cup \delta\Omega_n, \quad n = 1, 2, \ldots \end{aligned} \tag{22}$$

where $\delta\Omega_n = \{I \in \Lambda :\ u_I(hn) \in [0.4, 0.7],\ I \in \Gamma_n\}$.

The dynamical set Ω_n describes cells occupied by effective objects in the network space Λ at time n. It can only grow as the wavefront explores Λ. Then, we define:

$$q_I(\tau) = \begin{cases} 0, & \text{if } I \in \Omega_n \cup L \\ 1, & \text{otherwise.} \end{cases} \tag{23}$$

where $\tau \in [h(n-1)h, hn)$. Thus, cells in Ω_n have $du_I/d\tau = 0$ for $\tau \ge hn$ [see Eq. (19)] and hence will exhibit no dynamics in forward time, i.e., the effective objects are *static* and the wavefront slips around them (Figs. 2B, $\tau = 120$ and $\tau = 200$).

C. Motor Execution. Versatile Kicking the Ball

Once the wave has explored the handspace, we get a potential field (21) and effective static objects (see Figs. 2 and 3, respectively). These taken together represent a Generalized Cognitive Map of the situation. The effective objects contain critical information about possible collisions of the limb with

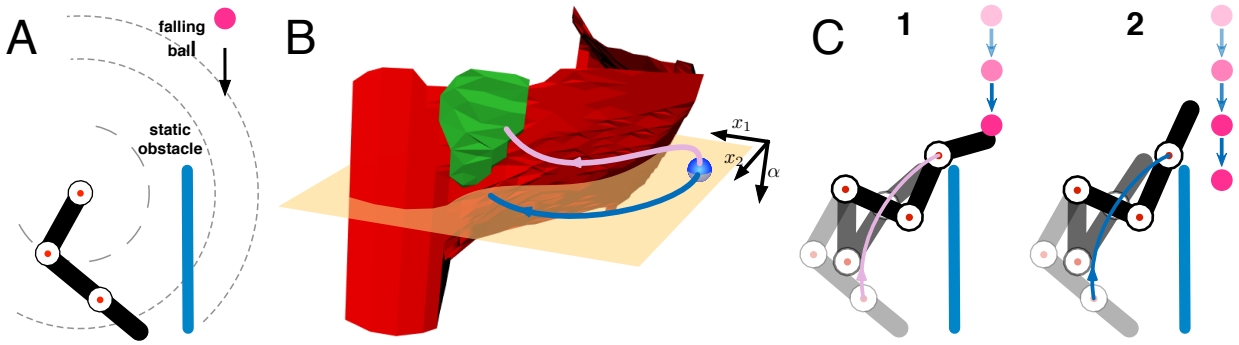

Fig. 4. Advantage of a limb with 3-DoF vs 2-DoF. A) Situation similar to Fig. 2A but now with an extra obstacle (blue bar) that "hides" the falling ball. B) Effective objects in the handspace $\mathcal{H}_3$. The obstacle is shown in red and the target in green. Yellow plane corresponds to $\alpha = 0$. Blue circle marks the initial position of the limb. To catch the ball it is necessary to bend the wrist joint (rose trajectory with decreasing $\alpha(\tau)$. Blue trajectory in the plane $\alpha = 0$ fails to reach the target. C) Examples of motor execution of trajectories shown in (B). In the case of a limb with flexible wrist, the ball can be caught (panel 1), whereas the 2-DoF limb fails to reach the target (panel 2).

the objects in the workspace. The gradient profile of the potential field ∇G imposes rules the limb should follow to reach the target.

We thus use a gradient descend method to find feasible trajectories connecting positions of the effective target and the initial location of the limb $I_h(0)$. Figures 3A and 3B (arrowed curves) show three representative examples of the trajectories. By construction of the field with a wavefront, such trajectories circumvent effective obstacles in the handspace. However, what is more important, if the limb follows one of the trajectories in the workspace [11]:

- The hand will reach the target;
- During the move, the limb (forearm and upper arm) will not bump against obstacles.

Therefore, in order to actuate in a given dynamic situation, we use one of the trajectories obtained in the handspace. Figure 3C shows examples of the motor execution in the workspace. In both cases, the limb successfully accomplishes the task "reach the target and avoid collisions with obstacles", as expected. However, in the 2-DoF case the repertoire of possible angles of the hand when kicking the ball is very limited (panel 1 in Fig. 3C). Playing a game, the ball can be rebound to the "up-right". The handspace $\mathcal{H}_3$ provides significantly reacher dynamics. In this case, we can easily choose the desired kick angle by selecting the value $\alpha(\tau_{\text{end}})$. For example, Fig. 3C exemplifies two other choices that lead to kicks directed to the "up-left" and to the "right" (panels 2 and 3, respectively).

V. Object Catching in Presence of Obstacles

The dynamic situation described above was intentionally selected simple enough to gain clarity. Nevertheless, the discussed approach is aplicable to situations of arbitrary complexity. To illustrate the potential of the method, let us consider a situation similar to that shown in Fig. 2A, but now with an extra obstacle (Fig. 4A). In this case the falling ball is reachable by the limb during some time interval only. Then, it hides behind the blue bar.

We repeated simulations described in previous sections. Figure 4B shows the effective static objects in the handspace $\mathcal{H}_3$. Now the part corresponding to collisions with obstacles (marked in red) is much bigger than in Fig. 3B. We also notice that the target (in green) does not intersect the plane $\alpha = 0$ (shown in yellow). This means that there is no valid trajectory to the target in the case of the rigid wrist. A valid trajectory should necessarily change the hand angle $\alpha(t)$ (rose arrowed curve in Fig. 4B). Although there is no trajectory with $\alpha = 0$, we can find one that goes closely to the target (blue arrowed curve in Fig. 4B).

Figure 4C shows examples of motor execution of limb movements given by the trajectories shown in Fig. 4B. As expected the limb with 3DoF (panel 1) intercepts the ball, while the limb with 2-DoF fails.

VI. Conclusions

In this work, we have provided and numerically verified a novel approach that allows solving the problem of object handling and manipulation on an abstract cognitive level. We have introduced a neural network capable of creating generalized cognitive maps in the handspace of a limb. Then such maps can be used either for direct interaction with the environment or for building memories and learning [22], [27].

The discussed model generalizes the theoretical development of the effective obstacles proposed in [24], [25] for controlling limbs in dynamic situations. The proposed 3D neural network can be used for decision-making in problems of controlling limbs with both minimal and redundant numbers of DoF. Thus, the approach is scalable, which is crucial for implementation in humanoid robots. We also note that the model naturally enables biasing the efforts of reaching a target among different DoF. Such an ability is frequently observed in humans playing sport games.

Concluding, the theory of generalized cognitive maps provides a functional bridge between effective cognition, coping with direct interaction in a workspace, and abstract cognition, whose impact over subject's behavior is less immediate, but much more profound.

ACKNOWLEDGEMENT

This work was supported by the Spanish Ministry of Economy and Competitiveness under grant FIS2017-82900-P and by the Ministry of Education and Science of Russia under project 14.Y26.31.0022.

REFERENCES

[1] H. Choset, S. Hutchinson, K. Lynch, G. Kantor, W. Burgard, L. Kavraki, and S. Thrun, *Principles of robot motion: theory, algorithms, and implementation*. The MIT Press, 2005.

[2] R.V. Patel and F. Shadpey, *Control of Redundant Manipulators: Theory and Experiments.* Springer-Verlag Berlin Heidelberg, 2005.

[3] J. McIntyre, M. Zago, A. Berthoz, and F. Lacquaniti, Does the brain model newtons laws? *Nat. Neurosci.*, 4, 693-694, 2001.

[4] P. Dean, J. Porrill, C. Ekerot, and H. Jorntell, The cerebellar microcircuit as an adaptive filter: experimental and computational evidence. *Nat. Rev. Neurosci.*, 11, 3043, 2010.

[5] B. Schmidt and A. Redish, Navigation with a cognitive map. *Nat.*, 497, 4243, 2013.

[6] M.F. Land, Do we have an internal model of the outside world? *Phil. Trans. Royal Soc. B*, 369, 20130045, 2014.

[7] A. Terekhov and J. ORegan, Space as an invention of active agents. *Front. Robotics AI*, 3, 4, 2016.

[8] W. Noguchi, H. Iizuka, and M. Yamamoto, Cognitive map self-organization from subjective visuomotor experiences in a hierarchical recurrent neural network. *Adapt. Behav.*, 118, 2017.

[9] L. Pisella, H. Grea, C. Tilikete, A. Vighetto, M. Desmurget, G. Rode, D. Boisson, and Y. Rossetti, An automatic pilot for the hand in human posterior parietal cortex: toward reinterpreting optic ataxia. *Nat. Neurosci.*, 3, 729736, 2000.

[10] B. Tatler and M. Land, Vision and the representation of the surroundings in spatial memory. *Phil. Trans. Royal Soc. B*, 366, 596610, 2011.

[11] J. Villacorta-Atienza, M. Velarde, and V.A. Makarov, Compact internal representation of dynamic situations: Neural network implementing the causality principle. *Biological Cybernetics*, 103, 285297, 2010.

[12] O. Khatib, Real-Time Obstacle Avoidance for Manipulators and Mobile Robots. *Int. J. Robot. Res.* 5, 90, 1986.

[13] L. Sentis and O. Khatib, Synthesis of whole-body behaviors through hierarchical control of behavioral primitives. *Int. J. Humanoid Robot.*, 2, 505518, 2005.

[14] D. Seredynsk, K. Banachowicz, and T. Winiarski, Graph-based potential field for the end-effector control within the torque-based task hierarchy. *Proc. Int. Conf. Methods Models Autom. Robot.*, 2016.

[15] A.J. Ijspeert, J. Nakanishi, and S. Schaal, Learning attractor landscapes for learning motor primitives. *Adv. Neur. Inform. Process. Syst.*, 15471554, 2003.

[16] D.H. Park, H. Hoffmann, P. Pastor, and S. Schaal, Movement reproduction and obstacle avoidance with dynamic movement primitives and potential fields. *Proc. Int. Conf. Humanoid Robots*, 2008.

[17] C. Calvo Tapia, I.Y. Tyukin, and V.A. Makarov, Fast social-like learning of complex behaviors based on motor motifs. *Phys. Rev. E* (submitted), 2018.

[18] H. Reimann, I. Iossifidis, and G. Schoner, Autonomous movement generation for manipulators with multiple simultaneous constraints using the attractor dynamics approach. *IEEE Int. Conf. Robotics Autom.*, 5470-5477, 2011.

[19] S. Li, Y. Zhang, and L. Jin, Kinematic Control of Redundant Manipulators Using Neural Networks. *IEEE Tran. Neur. Netw. Lear. Syst.*, 28, 2243-2254, 2017.

[20] H. Sadjadian, H.D. Taghirad, and A. Fatehi, Neural networks approaches for computing the forward kinematics of a redundant parallel manipulator. *Int. J. Comput. Intell.*, 2, 4047, 2005.

[21] J.A. Villacorta-Atienza, C. Calvo, and V.A. Makarov, Prediction-for-compaction: Navigation in social environments using generalized cognitive maps. *Biological Cybernetics*, 109, 307320, 2015.

[22] J.A. Villacorta-Atienza and V.A. Makarov, Neural network architecture for cognitive navigation in dynamic environments. *IEEE Transactions on Neural Networks and Learning Systems*, 24, 20752087, 2013.

[23] C. Calvo, J.A. Villacorta-Atienza, V. Mironov, V. Gallego, and V.A. Makarov, Waves in isotropic totalistic cellular automata: Application to real-time robot navigation. *Advances in Complex Systems*, 19, 165001218, 2016.

[24] J.A. Villacorta-Atienza, C. Calvo, S. Lobov, and V.A. Makarov, Limb movement in dynamic situations based on generalized cognitive maps. *Mathematical Modelling of Natural Phenomena*, 12, 1529, 2017.

[25] C. Calvo, I. Kastalskiy, J.A. Villacorta-Atienza, M. Khoruzhko, and V.A. Makarov, Holistic model of cognitive limbs for dynamic situations. *Proc. Int. Cong. Neurotechnix*, 60-67, 2017.

[26] M. Spong, S. Hutchinson, and M. Vidyasagar, (2006). Robot modeling and control. Wiley, New York.

[27] I. Tyukin, A.N. Gorban, C. Calvo, J. Makarova, and V.A. Makarov, High-dimensional brain: A tool for encoding and rapid learning of memories by single neurons. *Bulletin of Mathematical Biology*, DOI: 10.1007/s11538-018-0415-5, 2018.